ELSEVIER
Available online at www.sciencedirect.com
ScienceDirect
Procedia Engineering 10 (2011) 1378–1383
Engineering
Procedia

ICM11

Indentation Fracture Toughness of Nanostruc[illegible]red Alumina – 13% Titania Coatings Deposi[illegible]d by Atmospheric Plasma Spray

A. Rico*, C. J. Múnez, J. Rodríg[illegible]

Materials Science and Engineering Department,Rey Juan Carlos Univers[illegible] Tulip[illegible] Móstoles 28[illegible]31, Spain

Abstract

Al_2O_3–13% TiO_2 nanostructured coatings, deposite[illegible] [illegible]gglomerate[illegible] nanoparticles as feeding powders, were studied. Indentation fracture toughness has been det[illegible]ined [illegible] coatings by means of depth sensing indentation. Results were compared to conventional coatings with [illegible]mila[illegible] [illegible]tion. The relevance of the nanostructure was analyzed. Substantially improved behavio[illegible] observ[illegible]e nanostructured coatings. Increments close to 40% in fracture toughness were measured. To[illegible] [illegible]echani[illegible] such as crack deflection by the microstructural features and compressive residual stresses fi[illegible] are tho[illegible]t to be r[illegible]onsible for the observed behaviour. A theoretical model describing these phenomena was ap[illegible] and [illegible]e agreement with experiments was achieved.

Keywords: Fracture toug[illegible]ess; de[illegible]sing indentation; Alumina – Titania coatings; Nanostructured coatings.

1. Introdu[illegible]on

Fr[illegible]re to[illegible]ess of [illegible]asma spray coatings is directly related to adherence between microstructural fe[illegible]res [illegible] 2]. C[illegible] [illegible]end to propagate through weak connections, such as the lamellae boundaries. [illegible]ence, f[illegible]cture toug[illegible]ess of coatings can be up to 50 % lower than that corresponding to ceramic bulk [illegible]teri[illegible]icular, alumina coatings exhibit a significant drawback regarding its brittleness. A[illegible]ingly, one of the most employed solutions is to deposit a tougher component together with alum[illegible] In this sense, alumina – titania coatings have been extensively used in applications requiring good t[illegible]ological and inertness properties. Titania has a lower melting point than alumina, which enhances the adherence, porosity and, finally, the fracture toughness of the coating.

The small volume of samples limits the use of conventional techniques to measure the coating fracture toughness. Indentation methods have been extensively employed to extract this property but there exist

* Corresponding author. Tel.: +34914888083; fax: +34914888150.
E-mail address: alvaro.rico@urjc.es.

Selection and peer-review under responsibility of ICM11 doi:10.1016/j.proeng.2011.04.229

several difficulties to obtain a coherent measure. Due to the heterogeneous microstructure of thermal spray coatings, observed crack patterns do not completely match to those necessary to apply equations developed in the literature.

There are several works focused on the fracture toughness of alumina – titania coatings. The addition of titania to alumina coatings improves their fracture toughness due to its minor melting point. The crack propagation resistance of the coating increases with the plasma gun because more dense coatings are obtained [3 – 5]. Jordan et al. studied the crack propagation resistance of conventional and nanostructured alumina – titania coatings [6, 8 – 10] deposited by atmospheric plasma spray. They found that the fracture toughness of the nanostructured coating depends on the plasma energy. The crack propagation resistance increase as the energy does. The interaction between cracks and microstructural features are also different in conventional and nanostructured alumina – titania coatings. In the conventional material, cracks propagate through the splat boundaries, while in the nanostructured coating several interactions can be detected. Partially melted zones embedded in the nanocoating [6 – 15] are able to arrest and deflect cracks, increasing the crack propagation resistance of the nanocoating. Nevertheless the toughening mechanisms are not clearly addressed. The interaction between cracks and microstructural features need to be enlightened to quantify and to clarify the toughening mechanisms operative in the nanostructured materials.

In this work, depth sensing indentation is employed to propagate cracks in the ceramic coatings (conventional and nanostructured). Fracture toughness is measured and interpreted in terms of the deflection mechanisms observed, but also depending on the residual stresses developed inside the material during the cooling stage at plasma spray process. Analytical models are used to analyze the toughening effects observed in the nanostructured coating.

2. Materials and Experimental

2.1 Materials

Al_2O_3–13 % TiO_2 coatings deposited on SAE–42[illegible] steel by atmospheric plasma sprayed were studied. Conventional coatings were fabricated from commercial powder METCO 130 provided by SULTZER METCO™. The average size of the particles is approximately 50 µm in diameter.

Nanostructured Al_2O_3–13 % TiO_2 coatings were prepared from agglomerates, supplied by INFRAMAT ADVANCED MATERIALS™. The agglomerates, comprising nanometric particles (Nanox™ S2613S) with average size of 200 nm, were prepared by spray drying. The difference between this powder and the conventional powder was in the particle size (average diameter of 30 µm) and the presence of small additions of ZrO_2 and CeO_2. These powders can be projected using conventional plasma gu[illegible]

2.2 *Depth sensing indentation.*

Samples were prepared in plan view from the as-sprayed coatings. Depth-sensing indentation tests were carried out using a diamond Berkovich indenter with a nominal edge radius of 100 nm. The experimental device was a Nanoindenter XP (MTS System Co.) equipped with a high load modulus. The nanoindenter applies a load via a calibrated electromagnetic coil with a resolution of 50 nN. The displacement of the indenter was measured using a capacitive transducer with a resolution of 0.01 nm.

To differentiate the values of indentation fracture toughness between microstructural features, K_c, a matrix of indentations (10 x 15) was made on a representative area of the sample. A maximum load of 1 N was applied, which is large enough to induce fracture around the imprint. The distance between the indentations was maintained at 20 µm. The usual procedure for determining the indentation fracture toughness [39] cannot be applied unless a regular crack pattern is developed. Unfortunately, a regular crack pattern did not develop with the nanostructured and conventional samples. Therefore, the indentation fracture toughness was calculated by following the method described in [40]. The coating failure is associated with pop-in events that appear as discontinuities in the loading curve. Th[illegible]re dissipated energy, U_{fr}, can be derived from the difference between the experimental c[illegible] and [illegible] hypothetical curve that is obtained in the absence of failure. After the indentation tests, th[illegible]ctured area A_{fr}, around the residual imprints was measured with SEM. Finally, the indentation frac[illegible]re t[illegible]ness, K_c, of the coating was calculated using the following equation:

$$K_c = \left[\frac{EU_{fr}}{(1-\nu^2)A_{fr}} \right] \quad (1)$$

E and ν are the Young's modulus and Poisson's ratio of the coat[illegible]g, resp[illegible]vely. A Poisson's ratio of 0.28 was used for all coatings.

3. Results

A detailed description about the microstruct[illegible]f the nano[illegible]d and conventional coatings was previously presented in [6-16]. In the same way [illegible] modulus and hardness of these materials, and their relation to microstructure were extensively [illegible]cusse[illegible]7]. For convenience of the reader, a brief summary of the microstructure has been included [illegible]e microstructure of the coating fabricated from nanopowders consists of two main z[illegible]igure 1[illegible]Splats formed by deposition of individual molten droplets generate a lamellar full[illegible]elted [illegible]tructure [illegible]M) which is typically obtained when thermal projection techniques are used. N[illegible]ertheles[illegible] partially [illegible]elted (PM) zones corresponding to the deposition of semi–molten droplets ret[illegible]ing [illegible]ina nanoparticles of the starting powders were also included in the coating. T[illegible] morpho[illegible]y and composition of the conventional coating, deposited from standard micrometric p[illegible]s, is simila[illegible] the FM zones showed in the nanostructured coating. The splat morphology, typical [illegible]ther[illegible] projected c[illegible]tings, is clearly observed in figure 1b.

3.1 *Indentat[illegible] fract[illegible] toughness*

A statistica[illegible]lysis w[illegible]carried out using fracture toughness values that were measured from the mat[illegible]dentat[illegible]s p[illegible]rmed on the coatings. The fracture toughness histogram is presented in Figure 2[illegible]

[illegible]o dis[illegible]utions were exhibited by the nanostructured coating, but a wide, single distribution was o[illegible] for [illegible]nventional material.

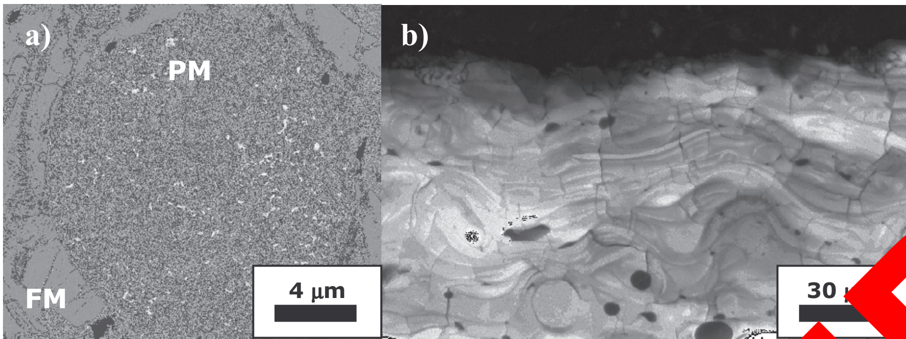

Figure 1. Microstructure of the coatings. a) Nanostructured. b) Conventional.

The PM domains appeared to be tougher than the FM regions in the nanostructured coating. Interestingly, the fracture toughness that was measured in the FM regions was also higher than the conventional coating, even when both are microstructurally equivalent [15].

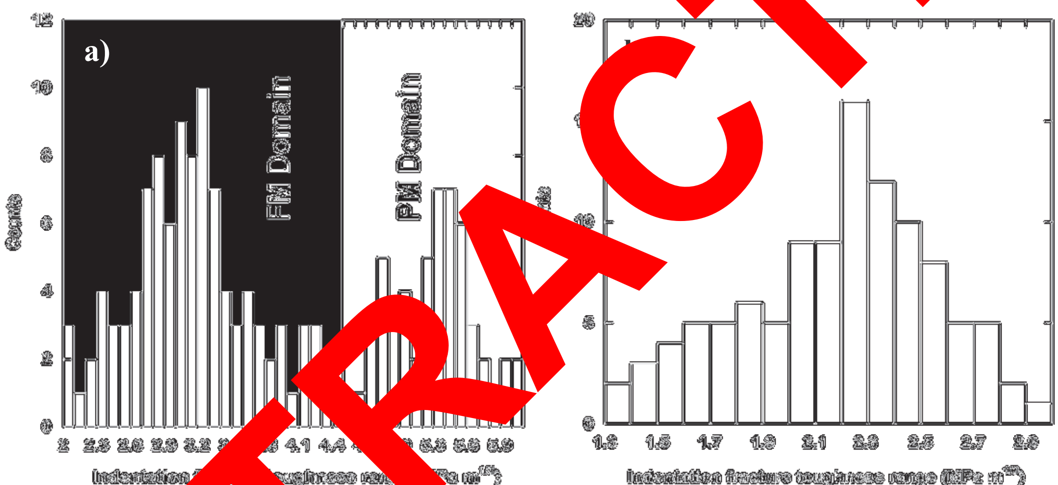

Figure 2. Indentation fracture toughness of the coatings. a) Nanostructured. b) Conventional.

Discussion

The hierarchical microstructure of the nanostructured coating seems to be responsible for the improvement in the fracture toughness. Traditionally, the toughening mechanisms encountered in ceramic matrix composites are: crack deflection by tough particles, crack bridging by ductile particles, crack bowing, fields of compressive residual stresses due to the manufacturing process and toughening transformations found in some ceramic materials such as ZrO_2. The high temperatures experienced by the nanocoating during plasma spraying, the subsequent fast cooling and the difference between the thermal expansion coefficients between the matrix (FM region) and the reinforcement (PM particles) induce compressive stress fields around the spherical particles which can affect the crack propagation. A model for the toughening increment by compressive residual stresses, ΔK_{RS}, was proposed by Evans et al. [17]

and also by Cutler and Virkar [18]. The model is based on a stress intensity factor solution by Tada et al. [19] for a semi–infinite two dimensional crack with a compressive stress zone of intensity q and length 2a. During the cooling stage, the compressive thermal residual stresses in the matrix are generated when the thermal expansion coefficient of the matrix exceeds that of the particle. Taya et al. modified this model to include the regular distribution of the particulate in the material [20]. The model, dependent on a, b, the inter-particulate spacing, and the local residual compressive stress around the spherical particle, q, can be expressed as follows:

$$\Delta K_{RS} = 2q\sqrt{\frac{2\cdot(b-2a)}{\pi}}$$

To estimate the compressive stresses an elastic model is used. If it is assumed that the matrix and the reinforcement exhibit elastic behaviour, then the residual thermal stress field between two reinforcement particles can be calculated. The maximum compressive stress corresponds to:

$$q = -\frac{P}{2}\left[1+\left(\frac{a}{a+b}\right)^{3}\right] \tag{4}$$

where:

$$P = \frac{(\alpha_m-\alpha_p)\cdot\Delta T\cdot E_m}{\frac{1-\upsilon_m}{2}+(1-2\upsilon_p)\cdot\frac{E_m}{E_c}} \tag{5}$$

To use the last equation, values for the thermal expansion coefficients of matrix ($\gamma - Al_2O_3$), α_m, and particles (75% α–Al_2O_3 and 25 % γ–Al_2O_3), α_p are required. The following data have been taken from the literature: $\alpha_p = 7{,}9\ 10^{-6}\ K^{-1}$ and $\alpha_m = 8$[illegible] K^{-1} [21]. Poisson coefficients for matrix, υ_m, and particle, υ_p, were considered to be 0,28 in both cases. It is not easy to estimate the temperature increment, ΔT, because of the temperature gradients within the plasma stream. As discussed, To include PM zones in the nanostructured coating, the temperature is maintained between the melting point, T_m, of the two components Al_2O_3 ($T_m \sim 2$[illegible] K) and TiO_2 ($T_m \sim 2123$ K).. However, many authors have pointed out that residual stresses are not induced in the material during the whole cooling stage. It is generally accepted that if temperature is above [illegible]0 % of the melting temperature, the material is able to accommodate the residual strain by means of creep phenomena. Below this temperature, residual stresses due to the mismatch between thermal expansion coefficients are generated. In addition, if particles are not completely molten during deposition (as it is the present case regarding the inclusion of partially melted particles in the coating) quenching of the liquid melt of the matrix leads to additional compressive residual stresses contributing to the toughening mechanism described here. Taking into account this observation, ΔT can be computed as the difference between the 50-70 % of the mean temperature between melting points during the plasma spray, and the room temperature, giving the range $\Delta T \sim$ [-810, -[illegible]0] [illegible] equations (4) and (5), it is possible to calculate a range for the maximum compressive stress, q, [-96, -147] MPa. If these values are introduced in equation (3) together with the values of *a* and *b* previously used, a toughening increase range is then obtained, ΔK_{RS} = [0.62, 0.96] MPa $m^{1/2}$. This result justifies the experimental differences observed between Fully Melted zones in the nanostuctured coating and conventional one.

4. Conclusions

Indentation fracture toughness of Al_2O_3–13% TiO_2 plasma sprayed nanostructured and conventional coating was analyzed. A significant increase in indentation fracture toughness is observed in nanostructured coatings due to its hierarchical microstructure and to the role played by the partially melted particles. These particles operate as obstacles to the crack propagation. The main toughening mechanism has been identified: residual stresses field due to mismatch between the coeffi[illegible]nts of thermal expansion of matrix and particulates. An analytical model was applied and a goo[illegible] with experiments was observed.

Acknowledgement

Authors are indebted to Comunidad de Madrid for the financial support thro[illegible] prog[illegible] ESTRU[illegible]AT (S-0505/MAT/0077)

References

[1] F. Beltzung, G. Zambell, E. López. Thin Solid Films (1989) 919 – 926.
[2] Erickson L. C., Hawthorne H. M., Troczynski T. Wear 200[illegible]: 569 – 57[illegible]
[3] Normand B., Fervel V. Coddet C. Nikitine V. Surfac[illegible] Coatings Techn[illegible]ogy 2000; 123: 278 – 287.
[4] K. J. Niemi, P. M. Vuoristo, A. T. Mantyla. Proc. [illegible] Thermal [illegible]ray Conference. C. Berndt, T. Bernecki (Eds.) 7 – 11 June Anheim CA, ASM, Metals Park[illegible] (199[illegible]7 – 48.
[5] K. A. Khor, Z. L. Dong, C. H. Quek, P. Che[illegible] Mater. Sci. [illegible]281 (2000) 221.
[6] Shaw L.L. Goberman D. Ren R., Gell M., [illegible]ang Y., Xiao T. D., Strutt P. R. Surface and coatings Technology 2000; 130: 1 – 8.
[7] Wang Y., Jiang S. Wang M. Wang S. Xiao T. [illegible]utt P. R. Wear 2000; 237: 176 -185.
[8] Gell M., Jordan E. H., Sohn Y., [illegible] L., Xi[illegible].D. Surface and Coatings Technology 2001; 146 – 147: 48 -54.
[9] Jordan E. H., Gell M., Sohn [illegible] Shaw L., Jiang S., Wang M., Xiao T.D., Wang Y. Strutt P. Materials Science[illegible] Eng[illegible]ing 2001; A301: 80 – 89.
[10] Goberman D., Soh[illegible]H., Shaw [illegible]rdan E., Gell M. Acta Materialia 2002; 50: 1141 – 1152.
[11] Liu Y. Fischer [illegible] A. Surface[illegible]nd Coatings Technology 2003; 167: 68 – 76.
[12] Bansal P., P[illegible]lture N. P., [illegible]iliev A. Acta Materialia 2003; 51: 2959 – 2970.
[13] Lin X., Z[illegible] Y., Lee S. W., [illegible]g C. Journal of the European Ceramic Society 2004; 24: 627 – 634.
[14] Cao X[illegible], Vass[illegible]R., Schwartz S., Jungen W., Tietz F., Stöever D. Journal of the European Ceramic Society 20[illegible]20: [illegible]3 – 2439.
[15] H. Luo, [illegible]oberm[illegible]L. Shaw, M. Gell. Materials Science and Engineering A 346 (2003) 237 – 24[illegible]
[16] J. R[illegible]iguez, [illegible]co, E. Otero W. M. Rainforth. Acta Materialia. 57 (2009) 3148-3156.
[17] F[illegible]Evans A. G. Acta metallurgica 1983; 31: 565 – 576.
[18] [illegible]atler R. A. Virkar A. V. Journal of Material Science 1985; 20: 3557 – 3573.
[19] [illegible]da H., Paris P.C., Irwin G. R. The stress analysis of crack Handbook. Del Research Corp, Hellert[illegible], PA, 1973 p.3,7.
[20] Taya M., Hayashi S., Kobayashi A. S, Yoon H. S. Journal of the American Ceramic Society 1990; 73: 1382 – 1391.
[21] Rohan P., Neufuss K., Matejicek J., Dubský J., Prchlík L., Holzgartner C. Ceramics International 2007; 30: 597 – 603.